mathematics

Article

Research on the Dynamic Characteristics of the Double Slings System with Elastic Connection Considering Boundary Conditions

Xia Liao [1], Danhui Dan [1,2,*], Fei Han [3] and Rui Zhao [1]

[1] School of Civil Engineering and Architecture, Xinjiang University, Urumqi 830047, China
[2] School of Civil Engineering, Tongji University, 1239 Siping Road, Shanghai 200092, China
[3] School of Mechanics, Civil Engineering and Architecture, Northwestern Polytechnical University, Xi'an 710129, China
* Correspondence: dandanhui@tongji.edu.cn; Tel.: +86-13918075836

Abstract: As the length of single sling increases, double slings with transverse connections are gradually becoming one of the effective measures to control the undesirable vibration of single slings. In the analysis of the dynamic characteristics of the double sling system, this paper firstly deduces the dynamic stiffness matrix of the elastically connected double sling system by the dynamic stiffness method (DSM), solves the frequency equation evolved from the dynamic stiffness matrix by using the Wittrick-Williams (W-W) algorithm, and obtains the systematic analysis and calculation of the dynamic characteristics of the double sling system under arbitrary boundary conditions. Secondly, a complete and accurate analysis method of the dynamic characteristics of the double sling system is obtained by comprehensively considering the bending stiffness and boundary conditions of the sling, and the accuracy of the calculation can be verified by the actual measurement data. Finally, the best installation position and quantity of transverse sling clamps in the double sling system are obtained by the parametric analysis of transverse sling clamps. The analysis of this paper will provide a theoretical basis for the design and optimization of slings, and further promote the wide application of the double sling system.

Keywords: double sling system; dynamic stiffness method; W-W algorithm; parametric analysis

MSC: 37M99; 65M99

check for updates

Citation: Liao, X.; Dan, D.; Han, F.; Zhao, R. Research on the Dynamic Characteristics of the Double Slings System with Elastic Connection Considering Boundary Conditions. *Mathematics* **2022**, *10*, 3129. https://doi.org/10.3390/math10173129

Academic Editors: Wei Zhang, Yuxin Hao and Youhua Qian

Received: 5 August 2022
Accepted: 26 August 2022
Published: 1 September 2022

1. Introduction

Due to the increase of single sling length, the flexibility of the sling also increases, making its lateral stiffness and internal damping reduced, and it is susceptible to various environmental effects such as wind and rain coupling as well as moving loads, producing various types of vibration phenomena. In order to effectively control the vibration of slings, multiple slings at the same lifting point are usually connected with transverse tie rods or vibration damping frames, thus forming a synergistic working system [1]. However, the double sling-clamp system as a special sling system still lacks a detailed discussion on the mechanical and usable properties of the system, and its mechanical principle has not been fully analyzed. The existing studies mainly propose cable network analysis models for horizontal double-cable or stay double-cable of cable-stayed bridges [2–6], while there are still fewer cable network analysis models for suspension bridges with suspension cables. Although the two bridges are extremely similar in form, there are some differences in the composition of the cables. The former usually consists of two slings with different lengths and physical parameters, while the latter is composed of two cables with the same physical and geometric parameters, making it difficult to distinguish the target sling from the adjacent sling. However, accurate analysis of the dynamic characteristics of the double sling system and study of the relevant factors affecting its dynamic characteristics are of great significance in guiding the design of the double sling system, monitoring during use, and maintenance of the sling at a later stage. Based on this, it is necessary to further research the dynamic characteristics of the double sling system.

In earlier studies, experimental and numerical simulation methods were usually used to study the mechanical properties of cable network systems. Yamaguchi [7,8] conducted an experimental study on free vibration of the double sling system connected by two cable clamps and investigated its intrinsic frequencies and vibration patterns as well as the control effect of sub-cables by means of a scaled model. Bosch [2] further used finite element software to simulate the mechanical properties of a sling system connected by cross-ties and obtained the performance of a set of diagonal cables connected by cross-ties, in which the effectiveness of the cross-ties depended on the geometry, number, size and anchorage conditions of their arrangement. Compared with experimental and numerical studies, numerical analysis can reveal the working mechanism of the double sling system more effectively [9]. Xu Hanzheng and Gan Quan [10,11] simplified the sling with a damping frame to the force model of a single sling under different constraints and loads, but the suspension bridge sling is actually a multi-cable system under the coupling of internal nodes, and its vibration is a comprehensive manifestation of the interaction of each cable, which is different from the vibration behavior of a single sling or a cable with good integrity. Caracoglia L [3–5] conducted a preliminary analysis of the natural vibration characteristics of double-layer and multi-layer cable networks connected by coupling; Ahmad J [12,13] further analyzed the natural vibration characteristics of a hybrid cable network system with coupled cable net and external damper; Sun L M and Zhou Yagang [6,14] applied the cable-spring-damper system model to the auxiliary cable of cable-stayed bridge and analyzed its damping mechanism; Chen Zhengqing [15] determined the dynamic characteristics of the sling and the damping scheme of the separator by the environmental excitation method and conducted a comparative study on the damping effect of the separator; considering the in-plane vibration of double strand sling, Li Shouying [16] deduced the motion differential equation when installing damper between double strands; Shan Deshan [17] established the motion differential equation of the sling with damping frame, and clarified the relationship between damping frame stiffness, sling force and its vibration frequency; Zhou H J [18–20] established a double tensioner-spring-damping system model, and analyzed the frequency and damping characteristics of the system free vibration.

As the suspension bridge slings are relatively shorter and stiffer than other cable structures such as cable-stayed, the influence of bending stiffness has a greater proportion. If the influence of bending stiffness is ignored when calculating the natural vibration characteristics of the coupled cable-stay system, the natural vibration frequency of the cable calculated by the theoretical formula will be smaller than the actual value, which will lead to a difference in the actual situation. Therefore, when studying the natural vibration characteristics of the coupled slings, it is necessary to consider the bending stiffness of the sling [21]. Chen Wei et al. [22] proposed a model of a double cable-strand coupled system considering the cable bending stiffness and deduced a theoretical formula for sling vibration; and the theoretical formula was verified using experimental and numerical analysis methods after solving for the sling natural vibration frequency, which paved the theoretical foundation for a comprehensive study of the double sling system. In a recent study, Jing [23] analyzed the dynamic characteristics of the cable network using uniformly distributed elastic cross-ties instead of the conventional single or multiple cross-ties. Lz A and Song Y A et al. [24] proposed the study on the dynamic characteristics of double slings considering the bending stiffness in their recent study, and the analysis of the slings' own parameters in the literature provided new ideas for this paper and the subsequent study of the dynamic characteristics of double slings. However, the boundary conditions of the double slings and the transverse sling clamps are only simply treated as rigid in the existing literature, ignoring the effect of the transverse sling clamps and the actual boundary conditions of the slings, as well as the influence of the boundary conditions on the dynamic characteristics of the double slings. For this reason, it is necessary to further integrate the sling boundary conditions for the analysis of the dynamic characteristics of the double sling.

Based on this, further dynamic characteristics of slings considering bending stiffness and boundary conditions will be carried out in this paper. In this paper, a double slings system with an elastic transverse cable clamp (hereinafter referred to as DSS-ETC) will be selected as the research object for further analysis, and the elastic transverse cable clamp in the double sling system is further analyzed in the form of sling boundary conditions. Firstly, the frequency equation considering the bending stiffness of the double sling system is derived from the differential equation controlling the free vibration in the plane, the frequency equation is solved and calculated by using the W-W algorithm [25], and the accuracy of the proposed system frequency equation analysis and calculation is verified by comparing the results with the results of existing literature results. Secondly, considering the effect of boundary conditions at both ends of the sling, a complete set of dynamic characteristic analysis methods for a double sling system can be obtained, which is verified by the measured data. Finally, based on the proposed frequency equation, the influence of the number and position of the clamps on the dynamic characteristics of DSS-ETC in the double sling-clamp system is analyzed to provide a theoretical basis for the wide application of the double sling system.

2. Dynamic Characteristic Analysis of the Double Sling System

2.1. Basic Assumptions and Frequency Equations

The following assumptions were made for the DSS-ETC in order to investigate the dynamic characteristics of the double slings system with the clamps.

a. The sling is idealized as tensioning cable;
b. Consider the bending stiffness of the sling system;
c. Neglect the additional cable force due to lateral vibration in the sling;
d. The material of the sling system is linear elastic as well as always in the range of linear elasticity during the vibration;
e. The strain of the sling is small and its cross-sectional size does not change;
f. The vibration of the sling only occurs in the transverse plane and its vertical axial vibration is ignored;
g. The change of the internal tension of the sling along the length of the sling is not considered;
h. The cable clamp is a linear elastic spring device;
i. The movement of the cable clamp is mainly longitudinal, and the transverse movement is ignored.

Based on the above assumptions, the basic analysis model of DSS-ETC with the clamps evenly dividing slings is established, as shown in Figure 1 below.

When the effects of the damping and shear of the sling are ignored, the general differential equation of the differential equation for the in-plane free vibration of the single sling can be directly obtained from the literature [26]. However, for the above-mentioned analysis model of the double sling system, in order to clearly express the specific situation of each sling section for subsequent analysis, the vibration differential equation can be further expressed with reference to the single sling as

$$E_i I_i \frac{\partial^4 u_{ij}(x_{ij},t)}{\partial {x_{ij}}^4} + m_i \frac{\partial^2 u_{ij}(x_{ij},t)}{\partial t^2} - H_i \frac{\partial^2 u_{ij}(x_{ij},t)}{\partial {x_{ij}}^2} - h_{ij}(t)\frac{d^2 y_{ij}(x_{ij})}{\partial {x_{ij}}^2} = 0 \tag{1}$$

where, i = 1, 2 is the sling number, j = 1, 2, 3, ... , n is the segment number of the sling, EI is the bending stiffness of the sling, and $u(x,t)$ is the transverse displacement function of the sling; H is the sling force; x for the distance of the sling from the upper end boundary; m is the mass per unit length of the sling; t is the vibration time, $h(t)$ is the additional force of the sling; $y(x)$ is the initial static configuration of the sling. Obviously, $u_{ij}(x_{ij}, t)$ is the transverse displacement function of the jth section of the sling of sling I.

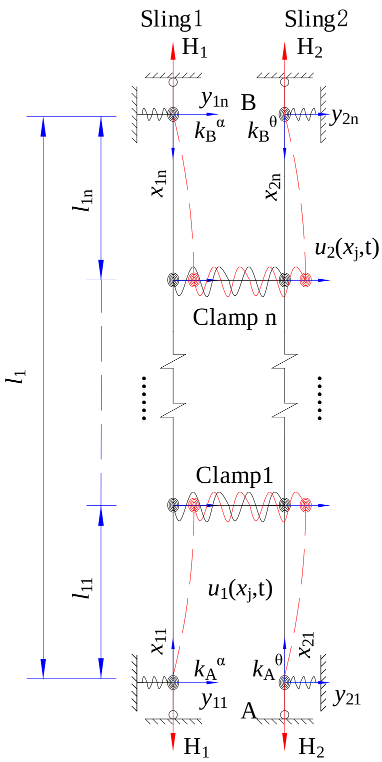

Figure 1. Analysis model of double slings system.

This paper aims to study the dynamic characteristics of vertical slings considering bending stiffness. Since the slings themselves are vertical and the transverse vibration of the slings is within a small range, the influence of the static configuration and the sag of the slings on the transverse vibration of the slings can be ignored, while the slings of specially designed arch bridges and suspension bridges need to be studied separately. Based on this, this paper will no longer consider the nonlinear term of the additional sling force, and Equation (1) can be further simplified as follows

$$E_i I_i \frac{\partial^4 u_{ij}(x_{ij}, t)}{\partial x_{ij}{}^4} + m_i \frac{\partial^2 u_{ij}(x_{ij}, t)}{\partial t^2} - H_i \frac{\partial^2 u_{ij}(x_{ij}, t)}{\partial x_{ij}{}^2} = 0 \tag{2}$$

According to the dynamic stiffness method (DSM) [27], it is assumed that

$$u_{ij}(x_{ij}, t) = \varphi_{ij}(x_{ij}) e^{i\omega t} \tag{3}$$

where, $\varphi_{ij}(x_{ij})$ is the mode shape function, ω is the circular frequency (rad/s), and t is the vibration time, $\sqrt{i^2} = -1$.

Introducing the dimensionless parameters: $\xi_{ij} = \frac{x_{ij}}{l_i}$, $\mu_{ij} = \frac{l_{ij}}{l_i}$, $\overline{\varphi}_{ij}(\xi_{ij}) = \frac{\varphi_{ij}(x_{ij})}{l_i{}^4}$, the dimensionless control differential equation of the system can be obtained by combining Equations (2) and (3).

$$\overline{\varphi}_{ij}(\xi_{ij})'''' - \gamma_i{}^2 \overline{\varphi}_{ij}(\xi_{ij})'' - \widetilde{\omega}^2 \overline{\varphi}_{ij}(\xi_{ij}) = 0 \tag{4}$$

where, $\gamma_i{}^2 = \dfrac{H_i l_i{}^2}{E_i I_i}$ is the ratio of the sling axial force to the bending stiffness value, $\widetilde{\omega} = \dfrac{\omega l_i{}^2}{\sqrt{E_i I_i / m_i}}$ is dimensionless frequency of the sling, and $\widetilde{\omega}^2 = \eta_i \omega^2$, $\eta_i = \dfrac{m_i l_i{}^4}{\sqrt{E_i I_i}}$.

Thus, the general solution of the differential Equation (4) can be expressed as

$$\overline{\varphi}_{ij}(\xi_{ij}) = \mathbf{\Phi}_{ij}(\xi_{ij})\left\{ A_{ij}{}^{(1)} \quad A_{ij}{}^{(2)} \quad A_{ij}{}^{(3)} \quad A_{ij}{}^{(4)} \right\}^T \tag{5}$$

where, $\mathbf{\Phi}_{ij}(\xi_{ij}) = \left\{ e^{-p_i \xi_{ij}} \quad e^{-p_i(1-\xi_{ij})} \quad \cos(q_i \xi_{ij}) \quad \sin(q_i \xi_{ij}) \right\}$, in which the specific expression of each element can be seen in Appendix A; $A_{ij}{}^{(1)} \sim A_{ij}{}^{(4)}$ is the coefficient to be determined with respect to the boundary conditions.

According to the relationship between nodal force and displacement functions in the sling system, the nodal displacements of the system characterized by the vibration mode function can be obtained as follows.

$$\begin{Bmatrix} \alpha_{aij} \\ \theta_{aij} l_i \\ \alpha_{bij} \\ \theta_{bij} l_i \end{Bmatrix} = \frac{l_i{}^4}{E_i I_i} \begin{Bmatrix} \overline{\varphi}_{ij}(\xi_{ij}|_{=0}) \\ \overline{\varphi}'_{ij}(\xi_{ij}|_{=0}) \\ \overline{\varphi}_{ij}(\xi_{ij}|_{=\mu_{ij}}). \\ \overline{\varphi}'_{ij}(\xi_{ij}|_{=\mu_{ij}}). \end{Bmatrix} = \frac{1}{\varsigma_i} \mathbf{G}_{ij} \begin{Bmatrix} A_{ij}{}^{(1)} \\ A_{ij}{}^{(2)} \\ A_{ij}{}^{(3)} \\ A_{ij}{}^{(4)} \end{Bmatrix} \tag{6}$$

where, $\varsigma_i = \dfrac{E_i I_i}{l_i{}^4}$, $\mathbf{G}_{ij} = \left\{ \mathbf{\Phi}_{ij}(\xi_{ij}|_{=0}) \quad \mathbf{\Phi}'_{ij}(\xi_{ij}|_{=0}) \quad \mathbf{\Phi}_{ij}(\xi_{ij}\big|_{=\mu_{ij}}) \quad \mathbf{\Phi}'_{ij}(\xi_{ij}\big|_{=\mu_{ij}}) \right\}^T$. The explicit expressions are given in Appendix A. α_{aij}, θ_{aij}, α_{bij} and θ_{bij} are the boundary line displacement and corner displacement near and far away from the lower end of the jth sling segment of sling i, respectively. The constant vector $\left\{ A_{ij}{}^{(1)} \quad A_{ij}{}^{(2)} \quad A_{ij}{}^{(3)} \quad A_{ij}{}^{(4)} \right\}^T$ can be expressed from Equation (6) as

$$\begin{Bmatrix} A_{ij}{}^{(1)} \\ A_{ij}{}^{(2)} \\ A_{ij}{}^{(3)} \\ A_{ij}{}^{(4)} \end{Bmatrix} = \varsigma_i \mathbf{G}_{ij}{}^{-1} \begin{Bmatrix} \alpha_{aij} \\ \theta_{aij} l_i \\ \alpha_{bij} \\ \theta_{bij} l_i \end{Bmatrix} \tag{7}$$

The relationship between its nodal force and displacement is

$$\begin{cases} V_{ij}(x_{ij}, t) = (E_i I_i \dfrac{\partial^3 \varphi_{ij}(x_{ij})}{\partial x_{ij}{}^3} - H_i \dfrac{\partial \varphi_{ij}(x_{ij})}{\partial x_{ij}}) e^{i\omega t} = l_i(\overline{\varphi}'''_{ij}(\xi_{ij}) - \gamma_i{}^2 \overline{\varphi}'_{ij}(\xi_{ij})) e^{i\omega t} \\ M_{ij}(x_{ij}, t) = E_i I_i \dfrac{\partial^2 \varphi_{ij}(x_{ij})}{\partial x_{ij}{}^2} e^{i\omega t} = l_i{}^2 \overline{\varphi}_{ij}''(\xi_{ij}) e^{i\omega t} \end{cases} \tag{8}$$

Combining Equations (6) and (7), we can obtain

$$\begin{Bmatrix} V_{aij} \\ M_{aij}/l_i \\ V_{bij} \\ M_{bij}/l_i \end{Bmatrix} = l_i \varsigma_i \mathbf{G}_{ij}{}^{-1} \begin{Bmatrix} \mathbf{\Phi}'''_{ij}(\xi_{ij}|_{=0}) - \gamma_i{}^2 \mathbf{\Phi}'_{ij}(\xi_{ij}|_{=0}) \\ -\mathbf{\Phi}''_{ij}(\xi_{ij}|_{=0}) \\ \mathbf{\Phi}'''_{ij}(\xi\big|_{=\mu_{ij}}) - \gamma_i{}^2 \mathbf{\Phi}'_{ij}(\xi_{ij}\big|_{=\mu_{ij}}) \\ -\mathbf{\Phi}''_{ij}(\xi_{ij}\big|_{=\mu_{ij}}) \end{Bmatrix} \begin{Bmatrix} \alpha_{aij} \\ \theta_{aij} l_i \\ \alpha_{bij} \\ \theta_{bij} l_i \end{Bmatrix} = l_i \varsigma_i \mathbf{D}_{ij} \mathbf{G}_{ij}{}^{-1} \begin{Bmatrix} \alpha_{aij} \\ \theta_{aij} l_i \\ \alpha_{bij} \\ \theta_{bij} l_i \end{Bmatrix} \tag{9}$$

where the specific explicit expressions are shown in Appendix A.

Then the dynamic stiffness matrix of the double slings system with the clamps can be obtained as

$$\mathbf{K} = l_i \varsigma_i \mathbf{D}_{ij} {\mathbf{G}_{ij}}^{-1} = \kappa_i \mathbf{D}_{ij} {\mathbf{G}_{ij}}^{-1} = \kappa_i \begin{pmatrix} {k_{11}}^{ij} & {k_{12}}^{ij} & {k_{13}}^{ij} & {k_{14}}^{ij} \\ {k_{21}}^{ij} & {k_{22}}^{ij} & {k_{23}}^{ij} & {k_{24}}^{ij} \\ {k_{31}}^{ij} & {k_{32}}^{ij} & {k_{33}}^{ij} & {k_{34}}^{ij} \\ {k_{41}}^{ij} & {k_{42}}^{ij} & {k_{43}}^{ij} & {k_{44}}^{ij} \end{pmatrix} \tag{10}$$

where, $\kappa_i = l_i \varsigma_i = \dfrac{E_i I_i}{{l_i}^3}$, the specific explicit expressions for each element are detailed in Appendix A.

2.2. Frequency Equation and Its Solution

Combining the boundary conditions of the force in the double sling system and Equation (10), the dynamic equilibrium equation of each sling segment in the double sling system can be obtained as follows.

$$\frac{E_i I_i}{{l_i}^3} \begin{pmatrix} {k_{11}}^{ij} & {k_{12}}^{ij} & {k_{13}}^{ij} & {k_{14}}^{ij} \\ {k_{12}}^{ij} & {k_{22}}^{ij} & -{k_{14}}^{ij} & {k_{24}}^{ij} \\ {k_{13}}^{ij} & -{k_{14}}^{ij} & {k_{11}}^{ij} & -{k_{12}}^{ij} \\ {k_{14}}^{ij} & {k_{24}}^{ij} & -{k_{12}}^{ij} & {k_{22}}^{ij} \end{pmatrix} \begin{Bmatrix} \alpha_{aij} \\ \theta_{aij} l_i \\ \alpha_{bij} \\ \theta_{bij} l_i \end{Bmatrix} = \begin{Bmatrix} {k_{aij}}^{\alpha} \alpha_{aij} \\ {k_{aij}}^{\theta} \theta_{aij} \\ {k_{bij}}^{\alpha} \alpha_{bij} \\ {k_{bij}}^{\theta} \theta_{bij} \end{Bmatrix} \tag{11}$$

where, ${k_{aij}}^{\alpha}$, ${k_{aij}}^{\theta}$, ${k_{bij}}^{\alpha}$ and ${k_{bij}}^{\theta}$ are the boundary line displacement stiffness and corner displacement stiffness of the j-th sling segment of sling i close to and away from the lower end, respectively. The specific expressions for each of element ${k_{ij}}^{ij}$ are detailed in Appendix A. By further matrix transformation, we can get

$$\frac{E_i I_i}{{l_i}^3} \begin{pmatrix} {k_{11}}^{ij} - \frac{l_i}{E_i I_i} {k_{aij}}^{\alpha} & {k_{12}}^{ij} & {k_{13}}^{ij} & {k_{14}}^{ij} \\ {k_{21}}^{ij} & {k_{22}}^{ij} - \frac{l_i}{E_i I_i} {k_{aij}}^{\theta} & {k_{23}}^{ij} & {k_{24}}^{ij} \\ {k_{31}}^{ij} & {k_{32}}^{ij} & {k_{33}}^{ij} - \frac{l_i}{E_i I_i} {k_{bij}}^{\alpha} & {k_{34}}^{ij} \\ {k_{41}}^{ij} & {k_{42}}^{ij} & {k_{43}}^{ij} & {k_{44}}^{ij} - \frac{l_i}{E_i I_i} {k_{bij}}^{\theta} \end{pmatrix} \begin{Bmatrix} \alpha_{aij} \\ \theta_{aij} l_i \\ \alpha_{bij} \\ \theta_{bij} l_i \end{Bmatrix} = \begin{Bmatrix} \mathbf{0} \\ \mathbf{0} \\ \mathbf{0} \\ \mathbf{0} \end{Bmatrix} \tag{12}$$

Then there is

$$\mathbf{K}(\omega) \begin{Bmatrix} \alpha_{aij} \\ \theta_{aij} l_i \\ \alpha_{bij} \\ \theta_{bij} l_i \end{Bmatrix} = \begin{Bmatrix} \mathbf{0} \\ \mathbf{0} \\ \mathbf{0} \\ \mathbf{0} \end{Bmatrix} \tag{13}$$

After obtaining the dynamic stiffness matrix of the double slings system with the clamps, the modal frequencies of each sling segment in the sling system can usually be solved by the following frequency equation.

$$|\mathbf{K}(\omega)| = 0 \tag{14}$$

where $|\cdot|$ represents the value of the determinant.

Equation (14) is the frequency equation of DSS-ETC. By solving Equation (14), the dynamic characteristics of each cable section in the DSS-ETC system can be analyzed. That is, the value satisfying the frequency equation of Equation (14) above is the modal frequency of each cable section of the sling system. The program is written by the W-W algorithm [25], and the calculation method of the frequency equation in the literature [28] is used to solve the dynamic characteristics.

2.3. Method Validation

In order to verify the accuracy of the model and calculation method proposed in this paper, the calculation results of the frequencies of each cable segment in the DSS-ETC are compared with the theoretical model proposed in reference [24] and the analytical method proposed in reference [12]. At the same time, parameter degradation of the theoretical hypothetical model in this chapter is required to unify the DSS-ETC model assumed in this paper with the models proposed in each piece of research literature.

The transverse elastic connection sling clamp in the single-clamp DSS-ETC is simplified to a rigid transverse rod, i.e., the single-clamp double sling system with rigid transverse connection (DSS-RTC), where the transverse connection transmits only shear force but not bending moment, and the sling clamp is connected at one-half of the length of the two slings, i.e., $\mu = 0.5$. Meanwhile, assuming that the parameters of the two slings in terms of mass, bending stiffness, and cross-sectional area are completely consistent, both ends of the slings are fixed supports, and the two slings are symmetrical about the cross-ties. Then, the simplified dynamic stiffness matrix of the double slings system in this paper can be obtained, and the frequency equation can be obtained as

$$\begin{vmatrix} {k_{11}}^{ij} & {k_{12}}^{ij} & {k_{13}}^{ij} & {k_{14}}^{ij} \\ {k_{21}}^{ij} & {k_{22}}^{ij} & {k_{23}}^{ij} & {k_{24}}^{ij} \\ {k_{31}}^{ij} & {k_{32}}^{ij} & {k_{33}}^{ij} & {k_{34}}^{ij} \\ {k_{41}}^{ij} & {k_{42}}^{ij} & {k_{43}}^{ij} & {k_{44}}^{ij} \end{vmatrix} = 0 \tag{15}$$

In the literature [29], the authors used the dynamic stiffness matrix to solve the frequencies of each order of the single-clamp double system with rigid transverse connections solidified at both ends of the sling, but the specific expressions of each element in the dynamic stiffness matrix were solved by the finite element method (shown Appendix A). The dynamic stiffness matrix is as follows

$$S = \begin{bmatrix} {k_{11}}^{(1)}(\mu_{11}) & {k_{11}}^{(2)}(\mu_{11}) & -{k_{12}}^{(1)}(\mu_{12}) & -{k_{12}}^{(2)}(\mu_{12}) & 0 & 0 & 0 & 0 \\ {k_{11}'}^{(1)}(\mu_{11}) & {k_{11}'}^{(2)}(\mu_{11}) & -{k_{12}'}^{(1)}(\mu_{12}) & -{k_{12}'}^{(2)}(\mu_{12}) & 0 & 0 & 0 & 0 \\ {k_{11}''}^{(1)}(\mu_{11}) & {k_{11}''}^{(2)}(\mu_{11}) & {k_{11}''}^{(1)}(\mu_{12}) & {k_{11}''}^{(2)}(\mu_{12}) & 0 & 0 & 0 & 0 \\ 0 & 0 & 0 & 0 & {k_{21}}^{(1)}(\mu_{21}) & {k_{21}}^{(2)}(\mu_{21}) & -{k_{22}}^{(1)}(\mu_{22}) & -{k_{22}}^{(2)}(\mu_{22}) \\ 0 & 0 & 0 & 0 & {k_{21}'}^{(1)}(\mu_{21}) & {k_{21}'}^{(2)}(\mu_{21}) & -{k_{22}'}^{(2)}(\mu_{22}) & -{k_{22}'}^{(2)}(\mu_{22}) \\ 0 & 0 & 0 & 0 & {k_{21}''}^{(1)}(\mu_{21}) & {k_{21}''}^{(2)}(\mu_{21}) & {k_{21}''}^{(1)}(\mu_{22}) & {k_{21}''}^{(2)}(\mu_{22}) \\ {k_{11}}^{(1)}(\mu_{11}) & {k_{11}}^{(2)}(\mu_{11}) & 0 & 0 & -{k_{21}}^{(1)}(\mu_{21}) & {k_{21}}^{(2)}(\mu_{21}) & 0 & 0 \\ {\delta_{11}}^{(1)} & {\delta_{11}}^{(2)} & {\delta_{12}}^{(1)} & {\delta_{12}}^{(2)} & {\delta_{21}}^{(1)} & {\delta_{21}}^{(2)} & {\delta_{22}}^{(1)} & {\delta_{22}}^{(2)} \end{bmatrix} \tag{16}$$

where, S is the dynamic stiffness matrix of the single-clamp double system with rigid transverse connections, and the specific expressions of the elements in the stiffness matrix are shown in Appendix A. In order to obtain the frequency of each cable section of the system, it is only necessary to solve the following frequency equation.

$$|S| = 0 \tag{17}$$

In reference [4], the author adopts the finite element analysis and calculation method. The sling parameters used in the numerical verification are those of the sling system used in reference [4], and the parameters are listed as shown in Table 1. However, the influence of the sling's own stiffness was not considered in that literature, i.e., the two parameters E and I were not used in the reference. In order to make a unified comparison of the results, the I parameter in the table is the minimum value that can be calculated by the method proposed in the literature.

Table 1. Sling parameters.

Parameter Symbols	$H_{1,2}$ (kN)	$m_{1,2}$ (kg/m)	$l_{1,2}$ (m)	$\mu_{1,2}$	$E_{1,2}$ (MPa)	$I_{1,2}$ (m^4)
Values	1598	47.9	67.34	0.5	195	2.260×10^{-9}

The frequency equations obtained using the analytical method in this paper were programmed by the W-W algorithm to calculate the frequency results of each cable segment in the single cable clamp DSS-RTC, compared with the results calculated by the method in each reference, as shown in Table 2.

Table 2. Frequency of each order for each sling section of the DSS-RTC with single sling clamp.

Modal Order	Frequency Calculation Value			Error Analysis		Modal Position
	Literature 1	Literature 2	This Paper	δ_1 (%)	δ_2 (%)	
1	1.3569	1.3563	1.3569	0.00	0.04	GM
2	2.7137	2.7126	2.7137	0.00	0.04	GM
3	2.7137	2.7126	2.7137	0.00	0.04	LM-US
4	2.7137	2.7126	2.7137	0.00	0.04	LM-LS
5	4.0706	4.0676	4.0706	0.00	0.07	GM
6	5.4274	5.4226	5.4274	0.00	0.09	GM
7	5.4274	5.4226	5.4274	0.00	0.09	LM-US
8	5.4274	5.4226	5.274	0.00	0.09	LM-LS
9	6.7843	6.7749	6.7843	0.00	0.14	GM
10	8.1412	8.1273	8.1412	0.00	0.17	GM

The following items need to be explained in Table 2.

(1) GM in the table represents the global mode of the sling, LM-US represents the local mode of the upper end of the sling, and LM-LS represents the local mode of the lower end of the sling.

(2) δ_1, δ_2 represents the relative error between the results calculated by the method in this paper and those calculated in literature 1 and 2, respectively, and the expression is $\delta = \left|\frac{\text{Calculation results in this paper } - \text{ Calculation results in literature}}{\text{Calculation results in literature}}\right|$.

(3) The calculation results of literature 1 are those in reference [24], where the calculation of the global mode of the sling is from the calculation method of literature [29], and the calculation results of literature 2 are using the finite element analysis method of reference [30], while the frequency of the global mode of the sling is calculated in this paper by using the method in literature [28].

In Table 2, comparing the frequency values of each sling segment in DSS-RTC with a single clamp obtained from each piece of the literature and the theoretical calculation in this paper, it is found that each order frequency values calculated by using the analytical calculation in this paper are exactly the same as the calculation results in literature 1, and the frequency error between the proposed method and literature 2 is also small enough to be negligible. The error is mainly due to the fact that the analytical calculation method proposed in this paper takes into account the bending stiffness of the double sling system, and the system stiffness of the single clamp DSS-RTC is greater than that in literature 2. Therefore, the frequency calculated by the method proposed in this chapter will be slightly larger accordingly. It is also shown that considering the bending stiffness of a single sling increases the system stiffness of the single clamp DSS-RTC. The error analysis verifies in both directions the accuracy of the theoretical analysis and calculation method of the modal frequencies of each order for each section of the single-clamp double sling system in this chapter. The method can be accurately applied to the analysis of the dynamic characteristics of the double sling system to provide an accurate theoretical basis for further parametric analysis and calculation of the double sling system.

2.4. Consideration and Verification of Boundary Conditions

The determination of the boundary conditions in the analysis and calculation of a single sling is proposed in the literature [25] and has been applied in engineering. The actual boundary conditions of the sling are determined from the parameters of the sling. The simply supported boundary can be used for the calculation at both ends of the sling of $l \geq 45\sqrt{\frac{EI}{H}}$; when $l \leq 15\sqrt{\frac{EI}{H}}$, the boundary conditions at both ends of the sling shall be treated as solid support boundary; when $15\sqrt{\frac{EI}{H}} \leq l \leq 45\sqrt{\frac{EI}{H}}$, the boundary at both ends of the sling shall be treated as an elastic complex boundary. The above conclusions will be applied to the sling system in DSS-ETC to determine the actual boundary conditions in the double sling system.

In order to verify whether the method of determining single sling boundary conditions can accurately reflect the actual boundary conditions of each sling in the double slings system, the measured dynamic characteristic data of the Yunnan Red River Special Bridge were selected for error analysis with the calculated frequencies of the double slings system in the case of double slings boundary conditions determined by applying the conclusions in the literature [28].

Engineering overview of the Red River Special Bridge, as shown in Figures 2 and 3: The Red River, with a total length of 1280 km, is an international river that spans China and Vietnam. The Red River Special Bridge is built to cross the Nansha Reservoir of the Red River and is the first highway suspension bridge across the Red River in China. The bridge is 1366 m long, of which the Jianshui bank approach bridge is 580 m long, the Yuanyang bank approach bridge is 80 m long and the main span is 700 m long. The main bridge of the bridge adopts a single span of 700 m simply supported steel box stiffening beam suspension bridge, and the main cable span is (310 + 700 + 175) m.

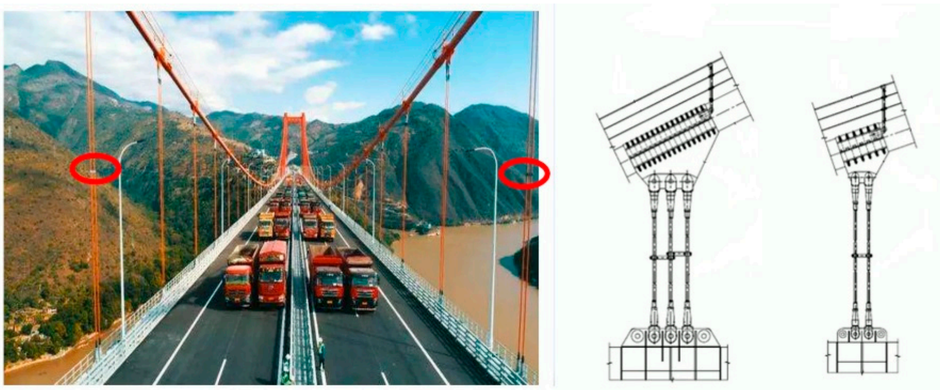

Figure 2. The double slings system of The Red River Special Bridge.

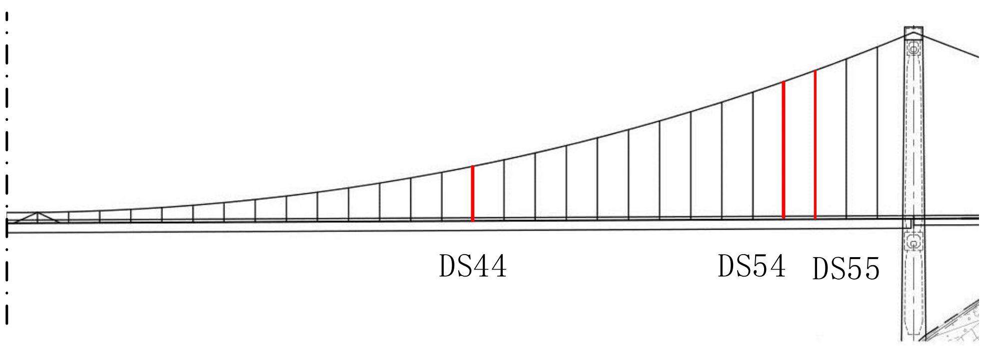

Figure 3. Half elevation of the Red River Special Bridge.

The DS44 and DS54 double slings systems in the Red River Special Bridge were selected as the research objects of this paper, which are double sling systems with evenly divided sling lengths for the single clamp device. As the difference of each sling length in the double slings system is negligible, it is assumed that the length of the single sling and other parameters in the double sling remains the same, and its main parameters are shown in Table 3. By installing the sensor device on the sling, the measured time and voltage are converted into the variation value of the vibration acceleration in the sling system with time. Further, the spectrum graph of the double slings system is obtained by fast Fourier transform (FFT), and the frequencies of each order in the vibration process of the sling system are finally obtained in the obtained spectrum graph. Based on the recording time of 120 s, the spectrum of the sling system and the frequency values of each order are obtained, as shown in Figures 4 and 5.

Table 3. Parameters of double slings system.

Sling Number	$H_{1,2}$ (kN)	$m_{1,2}$ (kg/m)	$l_{1,2}$ (m)	μ_{12}	$E_{1,2}$ (MPa)	$I_{1,2}$ (m^4)
DS44	500	12.75	19.44	1/2	200	7.73×10^{-7}
DS54	715	12.75	51.68	1/2	200	7.73×10^{-7}
DS55	750	12.75	55.82	1/3	200	7.73×10^{-7}

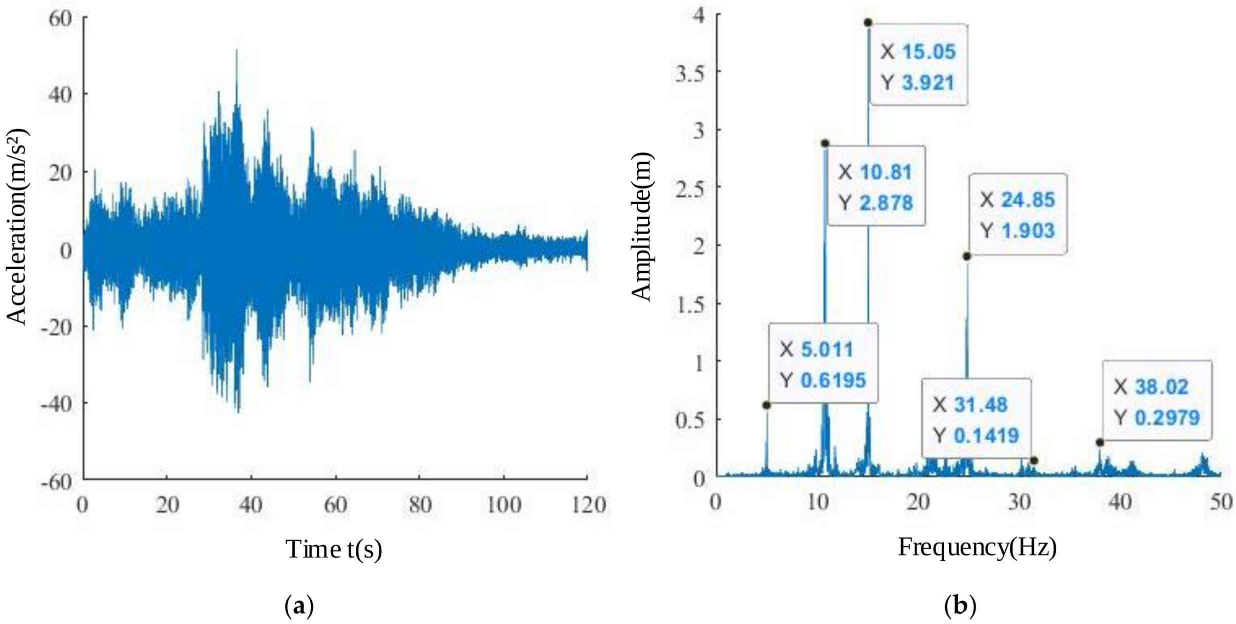

Figure 4. Frequency conversion diagram of DS44. (**a**) Acceleration variation graph. (**b**) Spectrogram.

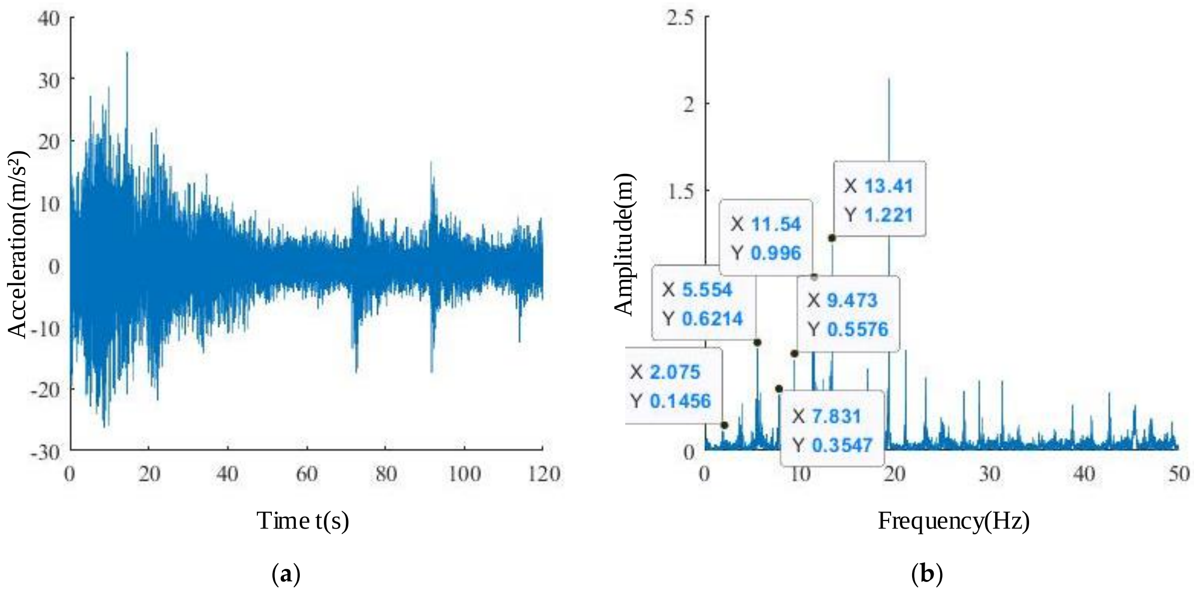

Figure 5. Frequency conversion diagram of DS54. (**a**) Acceleration variation graph. (**b**) Spectrogram.

Through the error analysis between the calculated frequency of the double sling system under the determined boundary conditions and the measured analysis value of the actual Red River Special Bridge, the application of the single sling boundary condition conclusions to the double sling system was verified. The two sling systems DS44 and DS54 with evenly divided sling lengths of transverse connection clamps in the Red River Special Bridge were selected as examples, and the first six order frequencies of the sling systems were calculated by combining the specific boundary conditions and the method of this paper, and the calculated frequencies of the sling systems were compared with the measured frequencies of the sling systems, as shown in Table 4 below. The relative error in the table is the absolute value of the relative error of the calculated frequency value of the sling relative to the measured frequency value.

Table 4. Frequency analysis of double slings system.

Modality	DS44			DS54		
	Measured Values (Hz)	Calculated Values (Hz)	Relative Errors (%)	Measured Values (Hz)	Calculated Values (Hz)	Relative Errors (%)
1st order	5.011	5.11	1.98	2.075	2.02	2.65
2nd order	10.81	10.35	4.26	5.554	5.37	3.31
3rd order	15.05	15.28	1.53	7.831	7.63	2.57
4th order	24.85	24.37	1.93	9.473	9.13	3.62
5th order	31.48	31.21	0.86	11.54	11.57	0.26
6th order	38.02	37.31	1.87	13.41	13.94	3.95

From Table 4 above, it can be seen that the maximum relative error between the measured value and the calculated frequency value of the double slings system evenly divided by transversely connected sling clamp does not exceed 4.26%, i.e., the sling frequency value obtained by the calculation method in this paper combined with the analysis of the boundary conditions of the single sling is not much different from the actual value of the project. The relative error analysis shows that the conclusions and definitions of the single sling boundary condition analysis are also applicable to the analysis of the dynamic characteristics of the double slings system, which means that the conclusions of the single sling boundary condition analysis can be applied to the calculation of the double slings system with certain accuracy. In the subsequent analysis of the dynamic characteristics of the double slings system, the single sling boundary conditions can be used to determine the boundary conditions of each sling section in the double slings system, so as to lay the boundary conditions foundation for the accurate analysis of the dynamic characteristics of the double slings system.

3. Influence of Sling Clamp Parameters on the Dynamic Characteristics of Double Slings System

3.1. Analysis of Sling Clamp Position

In order to study the influence of the transverse clamp position on the dynamic characteristics of the double slings system, the DHS_ECT system divided equally by the clamp is simplified accordingly, and only the influence of the different positions of the single clamp on the dynamic characteristics of the single-clamp DHS_ECT is considered. When analyzing the effect of transverse sling clamp position on the dynamic characteristics of the double slings system, the parameters of the slings in the system are set to be the same, and the parameters of the analyzed slings system are included in Table 5 as shown.

Table 5. Parameters of double slings system.

Parameter Symbol	$H_{1,2}$ (N)	$m_{1,2}$ (kg/m)	$l_{1,2}$ (m)	$\mu_{1,2}$	$E_{1,2}$ (MPa)	$I_{1,2}$ (m^4)
Value	1.5×10^6	45.7	20	0.5	195	2.260×10^{-6}

$15\sqrt{\frac{EI}{H}} = 8.13$ and $45\sqrt{\frac{EI}{H}} = 24.39$ can be obtained from the sling parameters of the parameters in the table. Under the consideration of the influence of the boundary conditions of the double slings system on the dynamic characteristics of the double slings, the first six order vibration frequency values of the double slings system at different sling clamp positions are calculated by using the analytical calculation method of this chapter. The transverse clamp position is transformed in the middle of the upper and lower boundaries of the sling, i.e., it changes in the middle of 0~l. In this section, the values of the transverse cable clamp positions are taken at a spacing of 0.1 l, 0.2 l, 0.3 l, ... , ... , 0.8 l, and 0.9 l, respectively. Based on the calculated frequency values of each order, the variation curve of each order frequency value of the double slings system with the position of the transverse cable clamp is drawn, as shown in Figure 6. At the same time, the first six frequency values of double slings when the transverse cable is clamped at 0.1 L, 0.2 L, and 0.5 L are listed in Table 6, and the corresponding frequencies of single slings are calculated for further analysis and comparison.

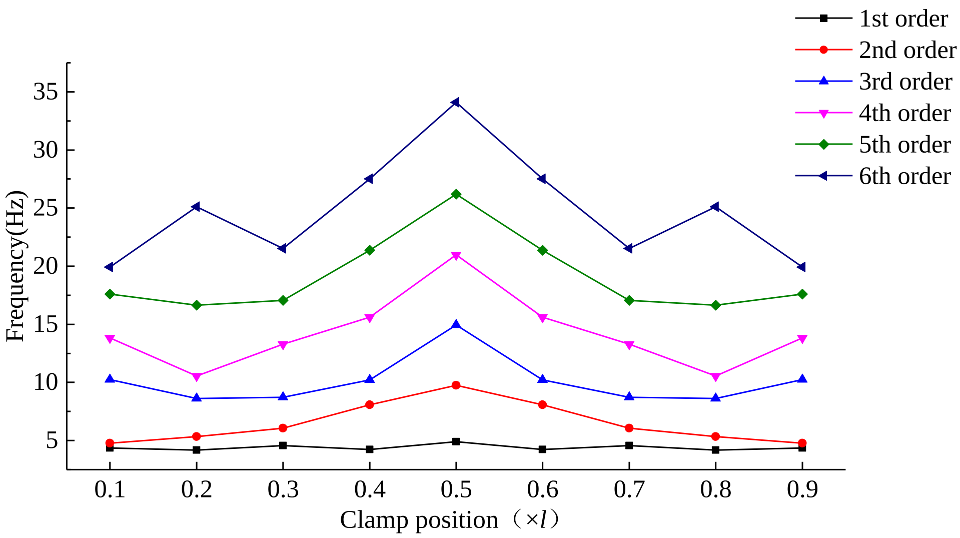

Figure 6. Variation of each order frequency of the double slings system with the position of the sling clamp.

Table 6. Frequency values of slings considering the position of the transverse sling clamp.

Sling Type	Clamp Position	Modal Frequency (Hz)					
		1st Order	2nd Order	3rd Order	4th Order	5th Order	6th Order
Double slings	0.1 l	4.36	4.78	10.24	13.84	17.59	19.92
	0.3 l	4.57	6.05	8.73	13.28	17.05	21.52
	0.5 l	4.91	9.76	14.94	20.99	26.19	34.09
Single sling		4.546	9.189	14.024	19.139	24.613	30.516

The parameters of the double sling system in Table 5 are from the literature [24], but the calculation results in this paper are somewhat different from those in the literature, mainly because this paper considers the influence of the boundary conditions of the sling on the dynamic characteristics of the sling, while the literature [29] assumes at the beginning that all the boundary conditions in the sling system are rigid connections.

The variation of the first six frequencies of the double slings system under different transverse sling clamp positions is shown in Figure 6. From the frequency change diagram of the sling system, it can be obtained that the transverse sling clamp position has a significant effect on the dynamic characteristics of DSS-ETC with the single sling clamp. Compared with the odd-order frequency, the even-order frequency fluctuates relatively more with the change of the transverse sling clamp position, i.e., the influence of the clamp position on the even-order frequency is more obvious, and this frequency change is more obvious with the increase of the frequency order. When the transverse sling clamp is located in the middle position of the sling, the frequency of each order of the sling in the double slings system reaches the peak.

As can be seen from the data in Table 6, when the transverse sling clamp is located near the middle of the sling, the frequencies of the double slings system are very close to those of the single sling. The frequencies of the double sling system at other transverse sling clamp installation locations are different from the calculated frequency values of the single sling because the adjacent frequency range of a single sling in a double sling system usually contains two system frequencies. In other words, when there is a transverse sling connection, in addition to the vibration of the single sling, other frequency components of vibration will be introduced. The reason for this is that the transverse clamps divide the sling into multiple sling segments which have local modal vibrations. However, when the transverse clamps are installed in the middle of the slings, i.e., the stationary point of the even-order vibration pattern, the effect of the transverse clamps on the dynamic characteristics of the slings in the double slings system can be basically negligible.

3.2. Quantitative Analysis of the Number of Sling Clamps

As the influence of single clamp position on the double slings system has been analyzed in the previous paper, in order to further study the influence of the number of clamps on the dynamic characteristics of the sling system in the double slings system with multi sling clamps, it is first assumed that the $(n-1)$ transverse clamps in the double slings system with multi sling clamp divide the length of a single sling into n segments, i.e., the length of each sling segment in the double slings system is the same. Take a certain double slings system a for the research object of the influence of the number of transverse clamps on its frequency, the main parameters of the double slings system are shown in Table 7.

Table 7. Parameters of double slings system.

Sling Number	$H_{1,2}$ (kN)	$m_{1,2}$ (kg/m)	$l_{1,2}$ (m)	μ_{12}	$E_{1,2}$ (MPa)	$I_{1,2}$ (m^4)
a	1500	45	20	1/n	195	6.24×10^{-6}

In order to calculate the effect of the clamp number on the dynamic characteristics of the multi-clamp double slings system, the transverse clamps were installed in the form of evenly divided sling lengths with 1, 2, and 3 . . . . . . 9 clamps, respectively. The frequency equation under consideration of boundary conditions is solved by programming with the W-W algorithm, and then each order frequency of each sling segments in the double slings system with different amounts of clamps are obtained, and the frequency values of each order of the corresponding single sling are calculated by using the calculation method in literature [28]. The frequency values of the double slings system varying with the number of transverse clamps when considering the actual boundary conditions of the sling are obtained from the calculations, as well as the frequency values of the corresponding single sling, as shown in Figure 7.

It can be obviously seen from Figure 7 that when the number of transverse clamps is 0 and 1, the sling frequency of each order basically does not change with the number of clamps, i.e., the frequency when the transverse clamp is installed in the middle position of the sling is basically the same as the frequency value of the single sling, and the transverse clamp installed only in the middle position of the sling does not affect the frequency of the single sling. This conclusion is consistent with the research conclusion of the effect of the single clamp position on the frequency of the double slings system in the previous section. In the double slings system, with the increase of the number of transverse clamps, the frequency value of each order of the sling gradually decreases. When the number of transverse clamps in the double slings system is n = 2, the change of the sling frequency value is the largest, which is obviously different from the double slings system with a single transverse clamp connected in the middle and the single sling without clamp connection. However, it can be seen from the figure that after the number of transverse clamps in the double slings system with multiple sling clamps is greater than two, the changes in each order frequency of double sling begin to stabilize, i.e., when the number of transverse clamps in double slings system is $(n-1) > 2$, the frequency of double slings system has little relationship with the number of transverse clamps in the system. Therefore, in practical engineering, we do not need to blindly increase the number of transverse clamps to control the vibration of the sling.

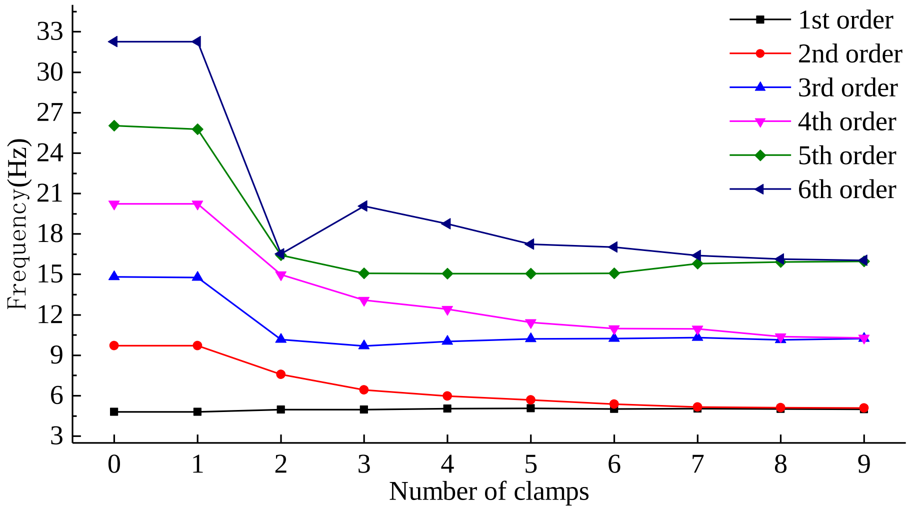

Figure 7. Variation diagram of each order frequency of double slings system a with the number of clamps.

4. Conclusions

In this paper, the dynamic characteristics of the double slings system are analyzed. Starting from the model of the double slings system, the dynamic stiffness matrix in DSS-ETC with single clamp and multi clamps is deduced by the dynamic stiffness method, and the frequency equation is solved by the W-W algorithm. At the same time, the boundary condition conclusions for a single sling are applied to the double slings system, and the accuracy of the dynamic characteristic calculation method in this paper when combined with the boundary conditions is further verified. In order to have a deeper understanding of the dynamic characteristics of the double slings system, parametric analyses are carried out for the transverse sling clamp positions and the number of transverse clamps in the double slings system, respectively. The main conclusions are as follows.

(1) The generalized frequency equations for double slings systems are deduced.

(2) In the double sling system, the parameters of each sling section can be used to determine the boundary conditions, both ends of the sling of $l \geq 45\sqrt{\frac{EI}{H}}$ can be calculated by simple supported boundary; when $l \leq 15\sqrt{\frac{EI}{H}}$, the boundary conditions at both ends of the sling shall be treated as solid support boundary; when $15\sqrt{\frac{EI}{H}} \leq l \leq 45\sqrt{\frac{EI}{H}}$, the boundary at both ends of the sling shall be treated as elastic complex boundary.

(3) When a transverse sling clamp is installed in the middle of the double slings system, the frequency value is basically the same as that of the single sling without the transverse clamp; when each sling in the double slings system is divided into three sections by two transverse clamps, the sling frequency is most obviously reduced; however, when the number of transverse clamps is greater than two, the number of transverse clamps has little effect on the frequency value in the double slings system.

Through the analysis of the dynamic characteristics of the double slings system with sling clamps, the systematic analysis theory of the dynamic characteristics of the double slings system and the analysis conclusion of sling parameters in the double slings system obtained in this paper provide a research means for the evaluation and analysis of the safety, suitability, and durability of large span bridges and provide a solid theoretical basis for the wide application of the double slings system in practical engineering.

Author Contributions: Conceptualization, D.D. and F.H.; methodology, X.L.; software, X.L. and R.Z.; validation, D.D., X.L. and F.H.; formal analysis, X.L.; investigation, X.L.; resources, D.D.; data curation, D.D., X.L. and F.H.; writing—original draft preparation, X.L.; writing—review and editing, D.D. and X.L.; visualization, X.L. and R.Z.; supervision, D.D. and F.H.; project administration, D.D.; funding acquisition, D.D. All authors have read and agreed to the published version of the manuscript.

Funding: This work was supported by the Xinjiang University Tianshan Scholar Distinguished Professor Research Start-up Fund (grant numbers 620312327).

Informed Consent Statement: Not applicable.

Data Availability Statement: Some or all data, models, or code that support the findings of this study are available from the corresponding author upon reasonable request.

Conflicts of Interest: The authors declare no conflict of interest.

Appendix A

$$\begin{aligned}
\mathbf{\Phi}_{ij}(\zeta_{ij}) &= \left\{ \begin{matrix} e^{-p_i\xi_{ij}} & e^{-p_i(1-\xi_{ij})} & \cos(q_i\xi_{ij}) & \sin(q_i\xi_{ij}) \end{matrix} \right\} \\
\mathbf{\Phi}_{ij}{}'(\zeta_{ij}) &= \left\{ \begin{matrix} -p_i\ e^{-p_i\xi_{ij}} & p_i e^{-p_i(1-\xi_{ij})} & -q_i\sin(q_i\xi_{ij}) & q_i\cos(q_i\xi_{ij}) \end{matrix} \right\} \\
\mathbf{\Phi}_{ij}{}''(\zeta_{ij}) &= \left\{ \begin{matrix} p_i{}^2\ e^{-p_i\xi_{ij}} & p_i{}^2 e^{-p_i(1-\xi_{ij})} & -q_i{}^2\cos(q_i\xi_{ij}) & -q_i{}^2\sin(q_i\xi_{ij}) \end{matrix} \right\} \\
\mathbf{\Phi}_{ij}{}'''(\zeta_{ij}) &= \left\{ \begin{matrix} -p_i{}^3\ e^{-p_i\xi_{ij}} & p_i{}^3 e^{-p_i(1-\xi_{ij})} & q_i{}^3\sin(q_i\xi_{ij}) & -q_i{}^3\cos(q_i\xi_{ij}) \end{matrix} \right\}
\end{aligned} \tag{A1}$$

where, $\left.\begin{matrix} p_i \\ q_i \end{matrix}\right\} = \sqrt{\sqrt{(\frac{\gamma_i}{2})^2 + \widetilde{\omega}^2} \pm \frac{\gamma_i{}^2}{2}} = \sqrt{\sqrt{(\frac{\gamma_i}{2})^2 + \eta_i\omega^2} \pm \frac{\gamma_i{}^2}{2}}$, $p_i{}^2 - q_i{}^2 = \gamma_i{}^2$, $p_i q_i = H_i\widetilde{\omega} = \pi\gamma_i\overline{\omega}$, $\overline{\omega} = \omega/\omega_0$, $\omega_0 = \dfrac{\pi}{l_i\sqrt{H_i/m_i}}$

$$\mathbf{G}_{ij} = \left\{ \begin{matrix} \mathbf{\Phi}_{ij}(\xi_{ij}|_{=0}) & \mathbf{\Phi'}_{ij}(\xi_{ij}|_{=0}) & \mathbf{\Phi}_{ij}(\xi_{ij}\big|_{=\mu_{ij}}) & \mathbf{\Phi'}_{ij}(\xi_{ij}\big|_{=\mu_{ij}}) \end{matrix} \right\}^T \tag{A2}$$

where
$$\begin{aligned}
\mathbf{\Phi}_{ij}(\xi_{ij}|_{=0}) &= \left\{ \begin{matrix} 1 & e^{-p_i} & 1 & 0 \end{matrix} \right\} \\
\mathbf{\Phi'}_{ij}(\xi_{ij}|_{=0}) &= \left\{ \begin{matrix} -p_i & p_i e^{-p_i} & 0 & q_i \end{matrix} \right\} \\
\mathbf{\Phi}_{ij}(\xi_{ij}|_{=\mu_{ij}}). &= \left\{ \begin{matrix} e^{-p_i\mu_{ij}} & e^{-p_i(1-\mu_{ij})} & \cos(q_i\mu_{ij}) & \sin(q_i\mu_{ij}) \end{matrix} \right\} \\
\mathbf{\Phi'}_{ij}(\xi_{ij}|_{=\mu_{ij}}). &= \left\{ \begin{matrix} -p_i e^{-p_i\mu_{ij}} & p_i e^{-p_i(1-\mu_{ij})} & -q_i\sin(q_i\mu_{ij}) & q_i\cos(q_i\mu_{ij}) \end{matrix} \right\}
\end{aligned}$$

$$\text{Namely } \mathbf{G}_{ij} = \begin{pmatrix} 1 & e^{-p_i} & 1 & 0 \\ -p_i & p_i e^{-p_i} & 0 & q_i \\ e^{-p_i\mu_{ij}} & e^{-p_i(1-\mu_{ij})} & \cos(q_i\mu_{ij}) & \sin(q_i\mu_{ij}) \\ -p_i e^{-p_i\mu_{ij}} & p_i e^{-p_i(1-\mu_{ij})} & -q_i\sin(q_i\mu_{ij}) & q_i\cos(q_i\mu_{ij}) \end{pmatrix}$$

$$\mathbf{D}_{ij} = \left\{ \begin{array}{l} \mathbf{\Phi'''}_{ij}(\xi_{ij}|_{=0}) - \gamma_i{}^2\mathbf{\Phi'}_{ij}(\xi_{ij}|_{=0}) \\ -\mathbf{\Phi''}_{ij}(\xi_{ij}|_{=0}) \\ \mathbf{\Phi'''}_{ij}(\xi|_{=\mu_{ij}}) - \gamma_i{}^2\mathbf{\Phi'}_{ij}(\xi_{ij}|_{=\mu_{ij}}).. \\ -\mathbf{\Phi''}_{ij}(\xi_{ij}|_{=\mu_{ij}}). \end{array} \right\} \tag{A3}$$

where

$$
\begin{aligned}
&\boldsymbol{\Phi}'''_{ij}(\xi_{ij}|_{=0}) - \gamma_i^2\boldsymbol{\Phi}'_{ij}(\xi_{ij}|_{=0}) = \{\ -p_i^3+\gamma_i^2 p_i \quad p_i^3 e^{-p_i}-\gamma_i^2 p_i \quad 0 \quad -q_i^3-\gamma_i^2 q_i\ \}\\
&-\boldsymbol{\Phi}''_{ij}(\xi_{ij}|_{=0}) = \{\ -p_i^2 \quad -p_i^2 e^{-p_i} \quad q_i^2 \quad 0\ \}\\
&\boldsymbol{\Phi}'''_{ij}(\xi|_{=\mu_{ij}}) - \gamma_i^2\boldsymbol{\Phi}'_{ij}(\xi_{ij}|_{=\mu_{ij}}).. = \Big\{ -p_i^3 e^{-p_i\mu_{ij}}+\gamma_i^2 p_i e^{-p_i\mu_{ij}} \quad p_i^3 e^{-p_i(1-\mu_{ij})}-\gamma_i^2 p_i e^{-p_i(1-\mu_{ij})}\ldots\\
&\ q_i^3\sin(q_i\mu_{ij})+\gamma_i^2 q_i\sin(q_i\mu_{ij}) \quad -q_i^3\cos(q_i\mu_{ij})-\gamma_i^2 q_i\cos(q_i\mu_{ij})\ \Big\}\\
&-\boldsymbol{\Phi}''_{ij}(\xi_{ij}|_{=\mu_{ij}}). = \Big\{\ -p_i^2 e^{-p_i\mu_{ij}} \quad -p_i^2 e^{-p_i(1-\mu_{ij})} \quad q_i^2\cos(q_i\mu_{ij}) \quad q_i^2\sin(q_i\mu_{ij})\ \Big\}\\
&k_{11}{}^{ij} = -p_i(p_i^2-\gamma_i^2)(c_{11}{}^{ij}-\varepsilon_{ij}c_{21}{}^{ij}) - q_i(q_i^2+\gamma_i^2)c_{41}{}^{ij} = -p_iq_i^2(c_{11}{}^{ij}-\varepsilon_{ij}c_{21}{}^{ij}) - q_ip_i^2c_{41}{}^{ij}\\
&k_{12}{}^{ij} = -p_i(p_i^2-\gamma_i^2)(c_{12}{}^{ij}-\varepsilon_{ij}c_{22}{}^{ij}) - q_i(q_i^2+\gamma_i^2)c_{42}{}^{ij} = -p_iq_i^2(c_{12}{}^{ij}-\varepsilon_{ij}c_{22}{}^{ij}) - q_ip_i^2c_{42}{}^{ij}\\
&k_{13}{}^{ij} = -p_i(p_i^2-\gamma_i^2)(c_{13}{}^{ij}-\varepsilon_{ij}c_{23}{}^{ij}) - q_i(q_i^2+\gamma_i^2)c_{43}{}^{ij} = -p_iq_i^2(c_{13}{}^{ij}-\varepsilon_{ij}c_{23}{}^{ij}) - q_ip_i^2c_{43}{}^{ij}\\
&k_{14}{}^{ij} = -p_i(p_i^2-\gamma_i^2)(c_{14}{}^{ij}-\varepsilon_{ij}c_{24}{}^{ij}) - q_i(q_i^2+\gamma_i^2)c_{44}{}^{ij} = -p_iq_i^2(c_{14}{}^{ij}-\varepsilon_{ij}c_{24}{}^{ij}) - q_ip_i^2c_{44}{}^{ij}\\
&k_{21}{}^{ij} = -p_i^2(c_{11}{}^{ij}+\varepsilon_{ij}c_{21}{}^{ij}) + q_i^2c_{31}{}^{ij},\ k_{22}{}^{ij} = -p_i^2(c_{12}{}^{ij}+\varepsilon_{ij}c_{22}{}^{ij}) + q_i^2c_{32}{}^{ij}\\
&k_{23}{}^{ij} = -p_i^2(c_{13}{}^{ij}+\varepsilon_{ij}c_{23}{}^{ij}) + q_i^2c_{33}{}^{ij},\ k_{24}{}^{ij} = -p_i^2(c_{14}{}^{ij}+\varepsilon_{ij}c_{24}{}^{ij}) + q_i^2c_{34}{}^{ij}\\
&k_{31}{}^{ij} = p_i\varepsilon_{ij}c_{11}{}^{ij}(p_i^2-\gamma_i^2) - p_ic_{21}{}^{ij}(p_i^2-\gamma_i^2) + (q_i^3+q_i\gamma_i^2)(-S_{ij}c_{31}{}^{ij}+C_{ij}c_{41}{}^{ij})\\
&= p_iq_i^2(\varepsilon_{ij}c_{11}{}^{ij}-c_{21}{}^{ij}) + q_ip_i^2(-S_{ij}c_{31}{}^{ij}+C_{ij}c_{41}{}^{ij})\\
&k_{32}{}^{ij} = p_i\varepsilon_{ij}c_{12}{}^{ij}(p_i^2-\gamma_i^2) - p_ic_{22}{}^{ij}(p_i^2-\gamma_i^2) + (q_i^3+q_i\gamma_i^2)(-S_{ij}c_{32}{}^{ij}+C_{ij}c_{42}{}^{ij})\\
&= p_iq_i^2(\varepsilon_{ij}c_{12}{}^{ij}-c_{22}{}^{ij}) + q_ip_i^2(-S_{ij}c_{32}{}^{ij}+C_{ij}c_{42}{}^{ij})\\
&k_{33}{}^{ij} = p_i\varepsilon_{ij}c_{13}{}^{ij}(p_i^2-\gamma_i^2) - p_ic_{23}{}^{ij}(p_i^2-\gamma_i^2) + (q_i^3+q_i\gamma_i^2)(-S_{ij}c_{33}{}^{ij}+C_{ij}c_{43}{}^{ij})\\
&= p_iq_i^2(\varepsilon_{ij}c_{13}{}^{ij}-c_{23}{}^{ij}) + q_ip_i^2(-S_{ij}c_{33}{}^{ij}+C_{ij}c_{43}{}^{ij})\\
&k_{34}{}^{ij} = p_i\varepsilon_{ij}c_{14}{}^{ij}(p_i^2-\gamma_i^2) - p_ic_{24}{}^{ij}(p_i^2-\gamma_i^2) + (q_i^3+q_i\gamma_i^2)(-S_{ij}c_{34}{}^{ij}+C_{ij}c_{44}{}^{ij})\\
&= p_iq_i^2(\varepsilon_{ij}c_{14}{}^{ij}-c_{24}{}^{ij}) + q_ip_i^2(-S_{ij}c_{34}{}^{ij}+C_{ij}c_{44}{}^{ij})\\
&k_{41}{}^{ij} = p_i^2(\varepsilon_{ij}c_{11}{}^{ij}+c_{21}{}^{ij}) - q_i^2(C_{ij}c_{31}{}^{ij}+S_{ij}c_{41}{}^{ij})k_{42}{}^{ij} = p_i^2(\varepsilon_{ij}c_{12}{}^{ij}+c_{22}{}^{ij}) - q_i^2(C_{ij}c_{32}{}^{ij}+S_{ij}c_{42}{}^{ij})\\
&k_{43}{}^{ij} = p_i^2(\varepsilon_{ij}c_{13}{}^{ij}+c_{23}{}^{ij}) - q_i^2(C_{ij}c_{33}{}^{ij}+S_{ij}c_{43}{}^{ij})k_{44}{}^{ij} = p_i^2(\varepsilon_{ij}c_{14}{}^{ij}+c_{24}{}^{ij}) - q_i^2(C_{ij}c_{34}{}^{ij}+S_{ij}c_{44}{}^{ij})
\end{aligned}
\tag{A4}
$$

where

$$
\begin{aligned}
&c_{11}{}^{ij} = -\frac{p_iq_iC_{ij}(C_{ij}\varepsilon_{ij}-1)+q_iS_{ij}+\varepsilon_{ij}p_iS_{ij}^2}{y_{ij}},\ c_{12}{}^{ij} = \frac{-p_iC_{ij}S_{ij}(C_{ij}\varepsilon_{ij}+1)+\varepsilon_{ij}p_iS_{ij}^2}{y_{ij}}\\
&c_{13}{}^{ij} = -\frac{q_i^2\varepsilon_{ij}S_{ij}-p_i(C_{ij}\varepsilon_{ij}-1)}{y_{ij}},\ c_{14}{}^{ij} = \frac{\varepsilon_{ij}q_iC_{ij}+\varepsilon_{ij}p_iS_{ij}-q_i}{y_{ij}}\\
&c_{21}{}^{ij} = \frac{q_i(C_{ij}^2-C_{ij}\varepsilon_{ij}+\varepsilon_{ij}q_iS_{ij}+p_iS_{ij}^2)}{y_{ij}},\ c_{22}{}^{ij} = \frac{q_iC_{ij}(C_{ij}-\varepsilon_{ij})+\varepsilon_{ij}p_iS_{ij}-q_iS_{ij}^2}{y_{ij}}\\
&c_{23}{}^{ij} = -\frac{p_iq_i(C_{ij}-\varepsilon_{ij})+q_i^2S_{ij}}{y_{ij}},\ c_{24}{}^{ij} = \frac{q_i(\varepsilon_{ij}-C_{ij})+p_iS_{ij}}{y_{ij}}\\
&c_{31}{}^{ij} = \frac{2\varepsilon_{ij}p_i-p_iq_iC_{ij}(1+\varepsilon_{ij}^2)-p_i^2S_{ij}(\varepsilon_{ij}^2-1)}{y_{ij}},\ c_{32}{}^{ij} = \frac{q_iC_{ij}(\varepsilon_{ij}^2-1)+p_iS_{ij}(1+\varepsilon_{ij}^2)}{y_{ij}}\\
&c_{33}{}^{ij} = \frac{-p_i+p_iq_i\varepsilon_{ij}C_{ij}(2-\varepsilon_{ij})}{y_{ij}},\ c_{34}{}^{ij} = \frac{p_i(1-\varepsilon_{ij}^2)-2p_i\varepsilon_{ij}S_{ij}}{y_{ij}}\\
&c_{41}{}^{ij} = \frac{p_iC_{ij}(1-\varepsilon_{ij}^2)+p_iq_iS_{ij}(1+\varepsilon_{ij}^2)}{y_{ij}},\ c_{42}{}^{ij} = \frac{p_i(2\varepsilon_{ij}-C_{ij}-C_{ij}\varepsilon_{ij}^2)+q_iS_{ij}(\varepsilon_{ij}^2-1)}{y_{ij}}\\
&c_{43}{}^{ij} = \frac{p_iq_i(\varepsilon_{ij}^2-2\varepsilon_{ij}S_{ij}-1)}{y_{ij}},\ c_{44}{}^{ij} = \frac{p_i(2\varepsilon_{ij}C_{ij}-\varepsilon_{ij}^2-1)}{y_{ij}}
\end{aligned}
$$

where, $\varepsilon_{ij} = e^{-p_i\mu_{ij}}$, $C_{ij} = \cos(q_i\mu_{ij})$, $S_{ij} = \sin(q_i\mu_{ij})$. $y_{ij} = 2p_iq_i(C_{ij}-\varepsilon_{ij})(\varepsilon_{ij}C_{ij}-1) - (\varepsilon_{ij}-1)S_{ij}(p_i^2-q_i^2+q_i^2\varepsilon_{ij}) + 2p_iq_i\varepsilon_{ij}S_{ij}^2$

$$
\begin{aligned}
&k_{ij}{}^{(1)}(\xi_{ij}) = e^{-p_i\xi_{ij}} - \cos(q_i\xi_{ij}) + \frac{p_i}{q_i}\sin(q_i\xi_{ij}),\ k_{ij}{}^{(2)}(\xi_{ij}) = (e^{-p_i\xi_{ij}} - \cos(q_i\xi_{ij}) - \frac{p_i}{q_i}\sin(q_i\xi_{ij}))e^{-p_i}\\
&k_{ij}{}'^{(1)}(\xi_{ij}) = -p_ie^{-p_i\xi_{ij}} + q_i\sin(q_i\xi_{ij}) + p_i\cos(q_i\xi_{ij}),\ k_{ij}{}'^{(2)}(\xi_{ij}) = (p_ie^{-p_i\xi_{ij}} + q_i\sin(q_i\xi_{ij}) - p_i\cos(q_i\xi_{ij}))e^{-p_i}\\
&k_{ij}{}''^{(1)}(\xi_{ij}) = p_i{}^2e^{-p_i\xi_{ij}} + q_i{}^2\cos(q_i\xi_{ij}) - p_iq_i\sin(q_i\xi_{ij})\\
&k_{ij}{}''^{(2)}(\xi_{ij}) = (p_i{}^2e^{-p_i\xi_{ij}} + q_i{}^2\cos(q_i\xi_{ij}) + p_iq_i\sin(q_i\xi_{ij}))e^{-p_i}\\
&k_{ij}{}'''^{(1)}(\xi_{ij}) = -p_i{}^3e^{-p_i\xi_{ij}} - q_i{}^3\sin(q_i\xi_{ij}) - p_iq_i{}^2\cos(q_i\xi_{ij})\\
&k_{ij}{}'''^{(2)}(\xi_{ij}) = (p_i{}^3e^{-p_i\xi_{ij}} - q_i{}^3\sin(q_i\xi_{ij}) - p_iq_i{}^2\cos(q_i\xi_{ij}))e^{-p_i}\\
&\delta_{ij}{}^{(1)} = k_{ij}{}'''^{(1)}(\xi_{ij}) - \gamma_i{}^2k_{ij}{}'^{(1)}(\xi_{ij}),\ \delta_{ij}{}^{(2)} = k_{ij}{}'''^{(2)}(\xi_{ij}) - \gamma_i{}^2k_{ij}{}'^{(2)}(\xi_{ij})
\end{aligned} \tag{A5}
$$

References

1. Ahmad, J.; Cheng, S. Effect of cross-link stiffness on the in-plane free vibration behaviour of a two-cable network. *Eng. Struct.* **2013**, *52*, 570–580. [CrossRef]
2. Bosch, H.R.; Pagenkopf, J.R. *Dynamic Properties of Stay Cables on the Penobscot Narrows Bridge*; Office of Infrastructure Research and Development, United States Federal Highway Administration: Mclean, VA, USA, 2014.
3. Caracoglia, L.; Jones, N.P. In-plane dynamic behavior of cable networks. Part 1: Formulation and basic solutions. *J. Sound Vib.* **2005**, *279*, 969–991. [CrossRef]
4. Caracoglia, L.; Jones, N.P. In-plane dynamic behavior of cable networks. Part 2: Prototype prediction and validation. *J. Sound Vib.* **2005**, *279*, 993–1014. [CrossRef]
5. Caracoglia, L.; Zuo, D. Effectiveness of cable networks of various configurations in suppressing stay-cable vibration. *Eng. Struct.* **2009**, *31*, 2851–2864. [CrossRef]
6. Zhou, Y.G.; Sun, L.M. Analysis and experiment on vibration control of stay cables with cross ties. In *Durability of Structure: SSCM'2006*; State Key Laboratory for Disaster Reduction in Civil Engineering, Tongji University: Shanghai, China, 2006.
7. Yamaguchi, H.; Nagahawatta, H.D. Damping effects of cable cross ties in cable-stayed bridges. *J. Wind. Eng. Ind. Aerodyn.* **1995**, *54*, 35–43. [CrossRef]
8. Yamaguchi, H.; Alauddin, M. Control of cable vibrations using secondary cable with special reference to nonlinearity and interaction. *Eng. Struct.* **2003**, *25*, 801–816. [CrossRef]
9. Krejsa, M.; Brozovsky, J.; Mikolasek, D.; Lehner, P.; Parenica, P. Using DOProC method in reliability assessment of steel elements exposed to fatigue. *MATEC Web Conf.* **2017**, *107*, 00046. [CrossRef]
10. Hanzheng, X.; Pingming, H. Research on sling force testing with vibration damping frame. *Highway* **2003**, *8*, 76–79.
11. Quan, G. Internal Force Identification Method for Cable Structures under Complex Boundary Conditions. Ph.D. Thesis, South China University of Technology, Guangzhou, China, 2015.
12. Ahmad, J. In-Plane Dynamic Behaviour of Conventional and Hybrid Cable Network Systems on Cable-Stayed Bridges. Ph.D. Thesis, University of Windsor, Windsor, ON, Canada, 2016.
13. Ahmad, J.; Cheng, S.; Ghrib, F. Combined effect of external damper and cross-tie on the modal response of hybrid two-cable networks. *J. Sound Vib.* **2018**, *417*, 132–148. [CrossRef]
14. Zhou, Y. Research on Dynamic Characteristics and Vibration Damping of Diagonal Cable-Assisted Cable System. Ph.D. Thesis, Tongji University, Shanghai, China, 2009.
15. Chen, Z.Q.; Lei, X.; Hua, X.G.; Li, S.Y.; Niu, H.W. Research and application of sling vibration reduction technology for long-span suspension bridges. *J. Hunan Univ. Nat. Sci. Ed.* **2016**, *43*, 10.
16. Li, S.; Zeng, Q.; Wang, S.; Zou, G.; Chen, Z. Theoretical study on the damping effect of dampers on double suspension cables of suspension bridge. *Eng. Mech.* **2018**, *35*, 8.
17. Shan, D.; Dong, J.; Liu, X.; Zhou, X.; Xu, L. Identification of cable force during suspender construction with vibration dampers. *Chin. J. Highw.* **2015**, *28*, 9.
18. Zhou, H.; Zhou, X.; Yao, G.; Sun, L.; Xing, F. Free vibration of two taut cables interconnected by a damper. *Struct. Control. Health Monit.* **2019**, *26*, e2423. [CrossRef]
19. Zhou, H.J.; Yang, X.; Pang, Y.R.; Zhou, R.; Sun, L.M.; Xing, F. Damping and frequency of twin-cables with a cross-link and a viscous damper. *Smart Struct. Syst.* **2019**, *23*, 669–682.
20. Zhou, H.J.; Wu, Y.H.; Li, L.X.; Sun, L.M.; Xing, F. Free vibrations of a two-cable network inter-supported by cross-links extended to ground. *Smart Struct. Syst.* **2019**, *23*, 653–667.
21. Wu, W.; He, X.; He, L.; Wu, C.; He, J.; Zhu, A. Joints Fatigue Damage Prediction for a Steel Truss Suspension Bridge Considering Corrosion Environment. *Arab. J. Sci. Eng.* **2022**, *47*, 4879–4892. [CrossRef]
22. Chen, W.; Wang, R.; Zhou, H.; Zhen, X.; Zhang, Z. Study on the natural vibration characteristics of coupled sling considering bending stiffness. *J. South China Univ. Technol. (Nat. Sci. Ed.)* **2020**, *48*, 143–154.

23. Jing, H.; He, X.; Zou, Y.; Wang, H. In-plane modal frequencies and mode shapes of two stay cables interconnected by uniformly distributed cross-ties. *J. Sound Vib.* **2018**, *417*, 38–55. [CrossRef]
24. Zhang, L.; Yang, S.; Chen, F.; Xu, B.; Dan, D. Parametric dynamic analysis of a double-hanger system via rigid cross-ties in suspension bridges. In *Structures*; Power China Roadbridge Group: Beijing, China, 2022; pp. 849–857.
25. Williams, F.W.; Wittrick, W. An automatic computational procedure for calculating natural frequencies of skeletal structures. *Int. J. Mech. Sci.* **1970**, *12*, 781–791. [CrossRef]
26. Humar, J. *Dynamics of Structure*; McGraw-Hill: New York, NY, USA, 1975.
27. Banerjee, J.R. Dynamic stiffness formulation for structural elements: A general approach. *Comput. Struct.* **1997**, *63*, 101–103. [CrossRef]
28. Dan, D.; Liao, X.; Han, F. Research on the Dynamic Characteristics of Cables Considering the Constraints at Both Ends of the Cables. *Appl. Sci.* **2022**, *12*, 2100. [CrossRef]
29. Xu, B.; Dan, D.; Zou, Y. Accurate identification method and practical formula of suspender tension based on tri-segment suspender dynamic model. *Eng. Struct.* **2019**, *200*, 109710.1–109710.11.
30. Ahmad, J.; Cheng, S. Analytical study on in-plane free vibration of a cable network with straight alignment rigid cross-ties. *J. Vib. Control* **2015**, *21*, 1299–1320. [CrossRef]